

Quantitative Myocardial Mapping of Perfusion and Metabolism Using Parametric Polar Map Displays in Cardiac PET

Paul K. Blanksma, Antoon T.M. Willemsen, Joan G. Meeder, Richard M. de Jong, Rutger L. Anthonio, Jan Pruim, Willem Vaalburg, Kong I. Lie

Department of Cardiology, University Hospital Groningen, PET Center, University Hospital Groningen, The Netherlands

Most efficacy studies of cardiac PET in demonstrating myocardial ischemia and viability have been performed using one or more transversal static images of the heart. In contrast, in this paper we describe a method of functional imaging of the complete left ventricular myocardium for perfusion with nitrogen-13-ammonia, both at rest and during a dipyridamol stress test, and of glucose metabolism with ^{18}F -fluorodeoxyglucose (^{18}F FDG). **Methods:** This was performed by using the data of each of 48 radial segments of 10 short-axis images as tissue data and LV cavity data of three basal planes as blood pool data. The study describes the results of 19 normal volunteers and 36 patients with coronary artery disease. From the data of the normal volunteers a 95% normal confidence interval was calculated for each imaging modality. These intervals were then used to describe the patient data as normal, ischemic or infarcted. **Results:** The results of analysis of the parametric images was compared with the results of static analysis of the same patient data and found to be less dependant on the detection threshold used. **Conclusion:** The described method enables the routine application of functional PET imaging of the total myocardium by the semi-automatic construction of parametric flow and metabolism polar maps. It thus provides an increased performance in the diagnosis, quantification and localization of myocardial ischemia and viability over conventional PET imaging.

Key Words: myocardial perfusion; parametric imaging; glucose metabolism

J Nucl Med 1995; 36:153–158

The use of PET for imaging myocardial perfusion and metabolism has been proven to be an accurate method for the study of myocardial ischemia and viability. It accurately predicts reversibility of myocardial function after revascularisation (1–3). Also, sensitivity and specificity of PET have been proven to be superior over thallium scintigraphy in assessing the presence, extent and localization of myocardial ischemia. However, it has not yet been

proven that the cost benefit ratio of the use of PET in patients with coronary artery disease is better than of that of ^{201}Tl or $^{99\text{m}}\text{Tc}$ -sestamibi. The use of ^{201}Tl reinjection techniques has recently been challenging PET as a method to demonstrate myocardial viability (4). Unfortunately, most of the older studies have been performed by PET cameras with 1 to 3 planes, using transversal PET images obtained in a static study (1) (one fixed frame). However, the main advantage of PET is its capability to quantitate metabolic processes by measuring the time course of blood and tissue data. In general, myocardial perfusion or glucose consumption is calculated by manual selection of a region of interest (ROI) in transversal images, which is not only time consuming but also discards the majority of the data. Therefore, an automatic routine by which quantitative dynamic images (parametric polar maps) can be obtained with complete three-dimensional imaging of the heart was developed. By comparing the results with 95% confidence limits of a normal population an objective measure of ischemic and infarcted myocardial regions is provided. We compared the results of our analysis method with an analysis of static data obtained in the same study.

METHODS

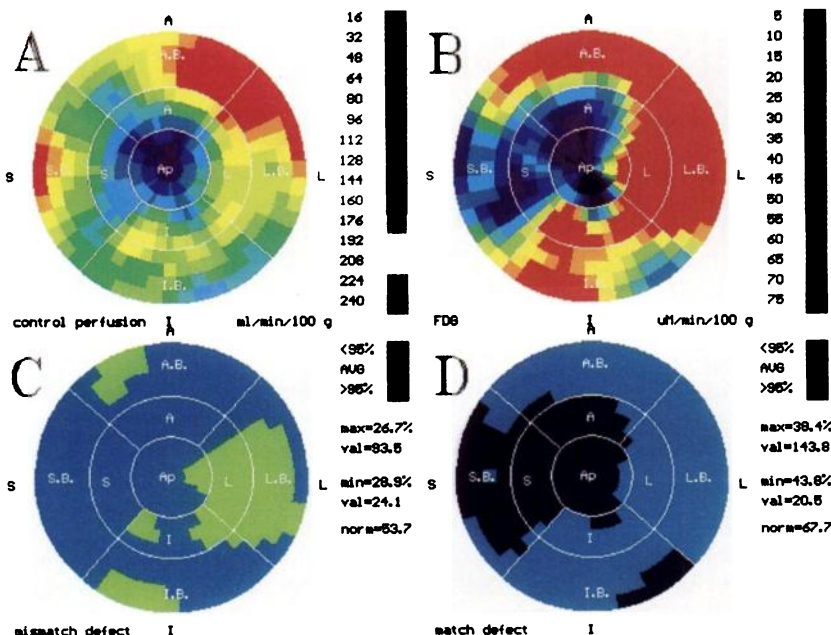
PET Data Acquisition

Myocardial perfusion was studied with the help of $^{13}\text{NH}_3$ and dynamic imaging of the heart according to the methods described by Schelbert and Phelps (5–7), and Bellina (8), in healthy volunteers and in patients with coronary artery disease. Subjects were positioned in a 951 Siemens positron camera imaging 31 planes simultaneously over 10.8 cm. Measured resolution of the system is 6 mm FWHM. Data was corrected for accidental coincidence and dead time automatically. Subjects were positioned with the help of a rectilinear scan. Photon attenuation was measured using a retractable external ring source filled with $^{68}\text{Ge}/^{68}\text{Ga}$. Dynamic imaging was started at the time of $^{13}\text{NH}_3$ injection (370 MBq) and was continued for 15 min (frames: 12×10 sec, 1×2 min, 1×4 min, 1×7 min). A control study was made, followed after 20 min by a provocation study with dipyridamol (DST). It was performed by injecting 0.56 mg dipyridamol/kg body weight over a 4-min interval. Nitrogen-13-ammonia-3 was injected 2 to 3 min after the end of the dipyridamol injection. During the procedure, heart rate and blood pressure were monitored continuously. After this, myo-

Received Dec. 17, 1993; revision accepted July 26, 1994.

For correspondence or reprints contact: Paul K. Blanksma, MD, Dept. of Cardiology, University Hospital Groningen, Oostersingel 59, P.O. Box 30.001, 9700 RB Groningen, The Netherlands.

FIGURE 1. Parametric polar maps of myocardial perfusion (A) and glucose consumption (B). The color scales pertinent to the maps are displayed to the right. In the bottom panel at left (C) the mismatch map is displayed as the ratio of B and A. In the map, the regions exceeding the 95% confidence interval are displayed in light green (increased ^{18}F uptake related to perfusion), the remainder in blue. At right, in the bottom panel (D) the match map is displayed. This is obtained by multiplying A and B and normalizing for mean flow (see text). The match defect is the region below the 95% confidence interval (concomitant low perfusion and ^{18}F uptake) and is displayed in black, the remainder in blue. At the right of the bottom maps the percentages of the myocardium in, below and above the 95% confidence interval and their values are indicated. This example is from a patient with extensive myocardial infarction in the anteroseptal region and ischemia in the posterolateral and inferior region.



cardiac glucose uptake was studied using ^{18}F FDG, using the methods of Krivokapich et al. (9) and Ratib et al. (10). Patients were studied after glucose loading with 50 g glucose orally administered, using a 17 frame protocol (8×15 sec, 4×30 sec, 1×1 min, 1×5 min, 1×10 min, 1×15 min, 1×20 min). The study was started 50 min after the last $^{13}\text{NH}_3$ study, when count rate had decreased below 2000 cps.

PET Data Analysis

The data of the $^{13}\text{NH}_3$ provocation study was corrected for remaining activity, by subtracting the last frame of the preceding study. The last frame of the preceding study was corrected to compensate for the decay between the two studies and then subtracted from all frames in the next study pixel by pixel. From previous studies the time-activity curves over a period of 40 min were available. These were used to estimate the maximum error due to this procedure, which was found to be less than 4% of the flow values. To further test the validity of this procedure, five volunteers were studied three times in succession without any intervention, with intervals of 20 min. The results were analyzed using the below mentioned method and compared. After this subtraction procedure, data for each study were reoriented to short-axis images using a manually drawn long-axis in the left ventricle. The myocardium in the different slices was divided into 48 segments (7.5° each). Using the maximum activity, time activity curves were established in all segments of all slices (11). A blood pool was defined in three slices near the base, the average of which was used to calculate a single blood-pool time-activity curve. For each segment the apparent myocardial flow was calculated as a function of time for a period of 120 sec. As this apparent flow time curve is noisy, an exponential fit was calculated and the flow was established at 90 sec. To compensate for flow-mediated extraction a correction was applied as given by Shah et al. (7):

$$E = E_0 \cdot (1 - 0.607 \cdot e^{-1.25/\text{Flow}}).$$

For calculation of glucose consumption, myocardial and blood-pool time-activity curves were used to perform a Patlak analysis

(9,10). Data obtained after 5 min postinjection were used to calculate the slope of the Patlak curve. So, for each individual segment myocardial perfusion and glucose consumption was calculated. From these data a parametric polar map was constructed, for the $^{13}\text{NH}_3$ perfusion studies using the perfusion model and for the ^{18}F -FDG studies using the Patlak analysis. From the perfusion maps of the control situation and from the provoked situation, perfusion ratio polar maps were constructed by calculating the ratio of the corresponding segments. To assess ischemia at rest, i.e., of hibernating myocardium, a ratio map was calculated of the ^{18}F FDG study and the resting perfusion study. For demonstrating provokable ischemia, the same was done for the ^{18}F -FDG study and the DST perfusion study. To allow further statistical analysis, the total myocardium was divided into nine regions (Fig. 1). Regional values were calculated for perfusion, perfusion ratio and glucose consumption. Each region was assumed to represent an equal part of the total myocardium, irrespective the number of segments in it.

For comparison with static imaging, the last frames of the $^{13}\text{NH}_3$ studies and the ^{18}F FDG studies were used. These data were normalized to a mean of 100%. After that, data analysis was performed in exactly the same way as for the parametric data.

From the normal volunteers data, we defined 95% confidence intervals of the normal values for each imaging modality for each myocardial segment (from mean $-2 \times$ the s.d. to mean $+2 \times$ the s.d. (10). Patients data then were compared to these intervals in each imaging modality, resulting in a 95% confidence map for each imaging modality. This indicates which myocardial segment is within, above or below the corresponding 95% confidence interval. In this way, per region calculations could be made of the percentage of myocardium above and below the 95% confidence interval, e.g., of the resting or provokable ischemic and infarct area. To quantify provokable ischemic myocardium, from the ratio map of ^{18}F FDG to dipyridamol stress test perfusion, the percentage myocardium above the 95% interval was calculated (mismatch defect calculation). To quantify infarcted, nonviable myocardium (match defect calculation) the ^{18}F FDG map was nor-

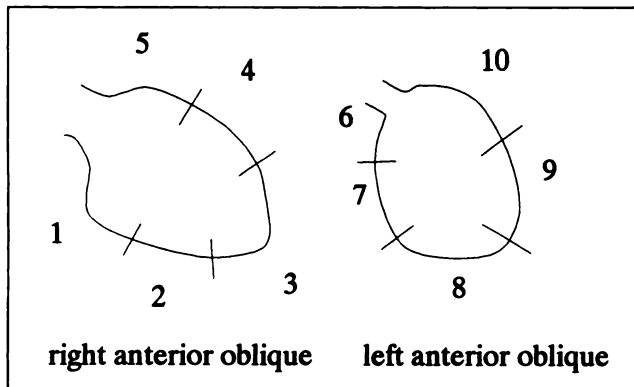


FIGURE 2. Regions of contrast ventriculography in the right anterior oblique 30° and left anterior oblique 60° projection.

malized for flow (viability = glucose uptake \times F_i/F_{mean} (F_i = segmental flow; F_{mean} = mean flow). From this match map the percentage myocardium below the 95% confidence interval was calculated (Fig. 1). The regional results were expressed as a percentage of the total myocardium, assuming that each region contained an equal part of the total myocardium.

Angiography

Left ventricular angiography was done in the right anterior oblique position (35° RAO) and left anterior oblique position (60° LAO). Coronary angiography was performed according to standard procedures in order to obtain projections of each major vascular segment in two perpendicular directions. The myocardium was divided in 5 regions in each projection (Fig. 2). A myocardial segment was considered to be infarcted if akinesia or dyskinesia was present. A myocardial segment was considered to be ischemic if the nutritive vessel showed a diameter narrowing of $\geq 50\%$.

VOLUNTEER STUDIES

Nineteen healthy volunteers were studied with $^{13}\text{NH}_3$. Data of five volunteers was used to assess both the short-term reproducibility as well as the feasibility of the correction for remaining activity. Ten volunteers underwent a control study and a dipyridamol stress test and seven volunteers underwent a study with ^{18}FDG . From the perfusion maps of the volunteers, regional values were calculated to study inhomogeneities, as reported by others (10). Short-term reproducibility was calculated by the s.d. of the percentage difference of the results of study number 1 and 2 and number 2 and 3. The systematic error produced by the subtraction of remaining activity was calculated from the percentage difference of the measurements. Finally, for all imaging modalities a 95% confidence interval was established from two s.d. below the mean value, found in the normal volunteers up to two s.d. above the mean.

PATIENT STUDIES

In a group of 36 consecutive patients (9 female and 27 male) with sustained myocardial infarction who were referred to establish the severity and localization of coronary artery disease and of myocardial viability, 40 studies were performed as described above. Mean age was 61.6 yr (ranging from 37 to 79 yr) In 4 patients the study was repeated after bypass surgery or balloon angioplasty. The results were compared with those of coronary

TABLE 1
Comparison of the Numbering of Myocardial Regions with PET and Angiography

PET	angiography
1. anterobasal	5
2. septobasal	6
3. inferobasal	1
4. laterobasal	10
5. anterior	4
6. septal	7
7. inferior	2
8. lateral	9
9. apical	3,8

In the angiography column, the numbers of the myocardial regions are given which are compared to the PET regions.

angiography ($n = 32$). Based on the anatomic localization of the myocardial regions of the different imaging techniques, these were considered to be corresponding regions according to Table 1. A per region comparison was made of ischemia and infarction separately. Angiographic infarction was assumed if the nutritive vessel was significantly ($>50\%$) narrowed and the LV wall was akinetic or dyskinetic. Angiographic ischemia was assumed if the nutritive vessel was significantly narrowed and the LV wall was hypo- or normokinetic. PET infarction was assumed if in the region more than $x\%$ of the total myocardium showed a matched defect, and PET ischemia was assumed if more than $x\%$ showed a mismatch defect. The value of x was used as a parameter of a ROC analysis, resulting in a predictive value for each percentage. Accordance of PET and angiography was assumed if both methods gave equal results in terms of normality, ischemia or infarction.

STATISTICS

For comparison of the results in PET and angiography a receiver operating characteristic (ROC) analysis was performed with the threshold myocardial percentage as parameter. For comparison of regional values of myocardial perfusion and glucose consumption a paired t-test was used. A probability value of 0.05 was considered to be significant.

RESULTS

Normal Volunteers

The results of the regional values of ^{18}FDG and $^{13}\text{NH}_3$ measurements are presented in Table 2. Control mean perfusion was 95.8 ± 5.0 ml/min/100 g, DST perfusion was 191.3 ± 15.3 ml/min/100 g, DST ratio was $196.0\% \pm 16.3\%$. Fluorine-18-FDG uptake was 54.8 ± 3.3 $\mu\text{mole/min/100 g}$. Small but significant differences were found between the myocardial regions. In the perfusion measurements, a tendency towards higher values was found in the inferior region, and a lower value in the apical region. In the ^{18}FDG measurements a tendency towards higher values was found in the lateral regions.

The results of the control study for the subtraction technique and reproducibility study of the $^{13}\text{NH}_3$ measure-

TABLE 2
Data of Regional Myocardial Perfusion at Rest and During a DST and Regional ^{18}F -FDG Uptake in Healthy Volunteers

	contr perf (ml/min/100 g)		DST perf (ml/min/100 g)		DST ratio (%)		FDG ($\mu\text{mole}/\text{min}/100\text{g}$)	
	mean	std.dev.	mean	std.dev.	Mean	std.dev.	mean	std.dev.
anbas	94.5	21.8	180.3	50.9	184.1	22.1	53.2	12.4
sepbas	96.9	18.4	179.9	46.5	173.1	16.4*	54.0	9.6
infbas	94.7	15.5	174.0	44.9	185.0	30.4	53.0	13.0
latbas	99.0	20.2	183.4	53.7	178.3	24.6	59.0	14.1*
ant	94.0	17.2	197.5	77.5	199.6	44.8	54.8	15.0
sept	97.5	19.3	195.8	60.1	207.2	31.3	56.2	13.5
inf	103.5	20.0*	222.3	71.3	220.8	46.2*	55.4	16.1
lat	96.8	16.8	204.7	67.4	207.1	42.0	59.3	19.2
api	85.0	18.5*	183.8	68.6	208.6	43.5	48.5	19.0
mean	95.8	18.6	191.3	60.1	196.0	33.5	54.8	14.7
std.dev.	5.0	1.9	15.3	11.7	16.3	11.0	3.3	3.1

*p < 0.05 vs. mean value.

ments are shown in Table 3. The mean percentual difference of the first and the second measurement was $5.9\% \pm 5.4\%$, of the second and the third measurement $3.5\% \pm 3.7\%$. This difference was not statistically significant. No systematic difference was found of the second and third subtracted and the first nonsubtracted studies and the random error was small.

Patients

The results of the ROC analysis of the static and the dynamic data of the patients are given in Figures 3 and 4. The optimal position of the predictive value was at a threshold of 2% to 3% of the myocardium for the static data and at 3% to 4% for the dynamic data and was 0.64 for both methods. When higher detection thresholds are used, static data have a lower predictive value than dynamic data.

DISCUSSION

The method of parametric imaging of myocardial perfusion measured with $^{13}\text{NH}_3$ PET and of myocardial glucose uptake measured with ^{18}F FDG PET described in this paper, provides an accurate and quantitative way to study the

condition of the myocardium in patients with coronary artery disease, both with and without previous infarction. The optimal predictive value of the dynamic data is equal to that of the static data, but it is less dependant on the threshold. This predictive value is relatively low (0.64), but it must be kept in mind that the test by which static and dynamic data were compared was a deliberately difficult one: the prediction of the presence of coronary artery disease was not tested, but the regional prediction of ischemia and infarction in patients with sustained myocardial infarction. Furthermore, angiography, although the de facto gold standard, is not an ideal method for discrimination of ischemia and infarction and PET has been shown to be superior in the past (1-3). The test was performed only to compare static and dynamic data.

The method to compare the results in patients with the

TABLE 3
Reproducibility Results in Five Normals Studied Three Successive Times

Patient no.	Study 1	Study 2	Study 3	% Difference for studies 1-2	% Difference for studies 2-3
1	87.7	92.2	97.4	4.9	5.3
2	95.2	92.7	93.0	-2.7	0.3
3	78.9	83.6	85.8	5.6	2.6
4	77.3	86.2	93.8	10.3	8.1
5	90.0	98.6	98.6	8.7	0.0
mean	85.8	90.7	93.7	5.4	3.3
std.dev.	7.6	5.9	5.0	5.0	3.4

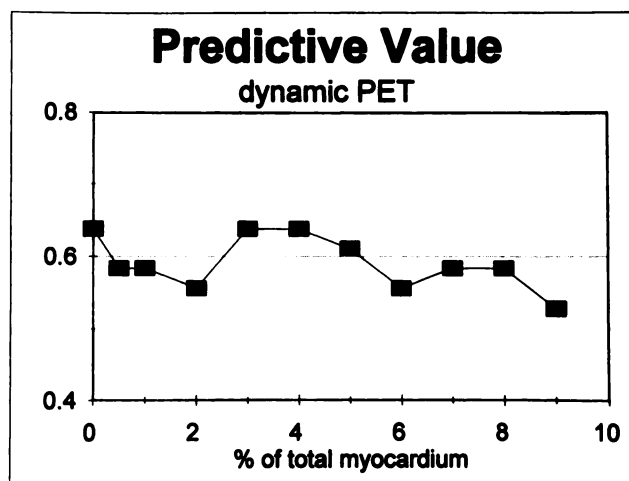


FIGURE 3. Plot of the predictive value of dynamic parametric PET as a function of the detection threshold. The predictive value is optimal for 3% to 4% of the total myocardium, but is relatively independent of it.

95% confidence intervals obtained in normal individuals provides a method to quantify the extent of myocardial ischemia and previous infarction as a percentage of the total myocardium. Consequently, this method enables us also to study quantitatively the influence of interventions on myocardial ischemia and infarct size.

The advantages of parametric imaging of perfusion over imaging of perfusion distribution from a static PET imaging are as follows:

1. Since an absolute value of myocardial perfusion is visualized in the image, instead of perfusion distribution, our methods allows direct identification of regions with increased as well as with decreased flow, as compared to normal. Patients with coronary artery disease, but also with other myocardial disorders (valvular disease, cardiomyopathy), often show an increased perfusion in normal myocardial areas, which can be interpreted as a sign of increased oxygen consumption due to myocardial overload. This provides extra information concerning the condition of the myocardium.
2. Perfusion distribution obtained from a static $^{13}\text{NH}_3$ image, which is usually acquired after a period of at least 4 min after tracer injection, does not only show $^{13}\text{NH}_3$ distribution, but also distribution of its metabolites, e.g., glutamate and urea which constitutes over 80% of ^{13}N activity in the plasma at this time (12). Consequently, static images acquired at this time do not necessarily reflect myocardial perfusion. As a matter of fact, an unexplained uneven distribution in static $^{13}\text{NH}_3$ studies in normal volunteers has been reported. A defect has been demonstrated in the posterolateral region in many healthy volunteers, impeding a proper interpretation of posterolateral defects in ten patients (10,13). In contrast, all defects found in normal volunteers could be explained from residual spillover effect of the liver (inferior region) and partial volume effects in the apical region. These effects may possibly be abolished by improvements of contour detection and myocardial recovery.
3. A major advantage over conventional PET is that parametric perfusion imaging obviates tedious ROI selection and separates perfusion calculations from PET studies and combines the advantages of PET imaging and perfusion calculations. Our method enables the detection of smaller regions of decreased as well as increased perfusion with the combination of static imaging and the calculation of separate ROI's.

The advantages of parametric imaging of ^{18}F FDG uptake have been described previously by Choi et al. (14). Because in regions with no active ^{18}F FDG uptake some activity is always present due to interstitial diffusion, contrast between viable and nonviable regions is diminished in static images. Because an increase of activity over the time of the study due to intracellular accumulation is accounted for only in parametric imaging, the signal is zero in infarcted

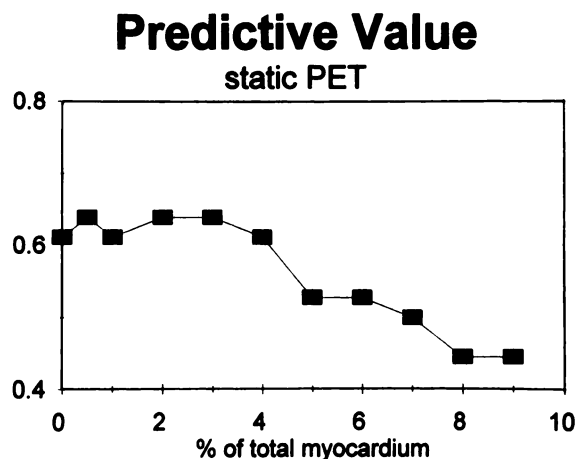


FIGURE 4. Plot of the predictive value of static PET as a function of the detection threshold. The value is optimal for a threshold of 2%–4% of the total myocardium and decreases rapidly from 5% upwards to 0.45.

regions (Fig. 1). This greatly enhances the diagnosis of previous infarction. Non-transmurally infarcted regions can be more easily discriminated from transmural infarctions with the help of parametric imaging.

Compared to previous reports on parametric imaging in PET, the advantages of displaying the results in a polar map are obvious (10). A more detailed and complete overview is obtained in a polar map of the myocardium than from transversal images. Also, the comparison with other imaging techniques (angiography, echocardiography) is easier and enables delineation of the complete flow region of the major coronary artery branches.

In conclusion, parametric display of myocardial perfusion with $^{13}\text{NH}_3$ and of glucose uptake with ^{18}F FDG is a new data analysis method in PET which is applicable with new high-resolution PET cameras. It provides a simple, sensitive and reliable method for the diagnosis, quantification and localization of myocardial regions with abnormally increased and decreased myocardial perfusion and viability, enabling an increased diagnostic power of PET in coronary artery disease and other myocardial diseases. Furthermore, the semi-automatic construction of parametric flow and metabolism polar maps of the total myocardium now enables the routine application of this technique in the clinical setting. The impact of the described method on the cost benefit ratio of clinical cardiac PET has yet to be established in prospective randomized studies.

REFERENCES

1. Tillisch J, Brunken R, Marshall R, et al. Reversibility of cardiac wall motion abnormalities predicted by PET. *New Engl J Med* 1986;314:884–8.
2. Brunken RC, Kottou S, Nienaber CA, Schwaiger M, Ratib OM, Phelps ME. PET detection of viable tissue in myocardial segments with persistent defects at Tl-201 SPECT. *Radiology* 1989;172:65–73.
3. Brunken RC, Tillisch J, Schwaiger M, Child JS, Marshall R, et al. Regional perfusion, glucose metabolism and wall motion in patients with chronic Q-wave infarction. *Circulation* 1986;73:951–963.
4. Dilsizian V, Rocco TP, Freedman NM, Leon MB, Bonow RO. Enhanced

- detection of ischemic but viable myocardium by the reinjection of thallium after stress-redistribution imaging. *N Engl J Med* 1990;323:141-146.
5. Schelbert HR, Phelps ME, Huang SC, et al. Nitrogen-13 ammonia as an indicator of myocardial blood flow. *Circulation* 1981;63:1259-72.
 6. Wisenberg G, Schelbert HR, Hoffman EJ, et al. In vivo quantification of regional myocardial blood flow by positron emission tomography. *Circulation* 1981;63:1248-1258.
 7. Shah A, Schelbert HR, Schwaiger M, et al. Measurement of regional myocardial blood flow with N-13 ammonia and positron emission tomography in intact dogs. *J Am Coll Cardiol* 1985;5:92-100.
 8. Bellina CR, Parodi O, Camici P, et al. Simultaneous in vitro and in vivo validation of nitrogen-13-ammonia for the assessment of regional myocardial blood flow. *J Nucl Med* 1990;31:1335-1343.
 9. Krivokapich J, Huang SC, Phelps ME, et al. Estimation of myocardial metabolic rate for glucose using fluorodeoxyglucose. *Am J Physiol* 1980; 238:E69.
 10. Ratib O, Phelps ME, Huang SC, Henze E, Sellin C, Schelbert HR. The deoxyglucose method for the estimation of local myocardial glucose metabolism with positron emission tomography. *J Nucl Med* 1982;23:577-586.
 11. Porenta G, Kuhle W, Czernin J, et al. Semiquantitative assessment of myocardial blood flow and viability using polar map displays of cardiac PET images. *J Nucl Med* 1992;33:1628-36.
 12. Rosenspire KC, Schwaiger M, Mangner ThJ, Hutchins GD, Sutrik A, Kuhl DE. Metabolic fate of [¹³N]ammonia in human and canine blood. *J Nucl Med* 1990;31:163-167.
 13. Laubenbacher C, Rothley J, Sitomer J, et al. An automated analysis program for the evaluation of cardiac PET studies: initial results in the detection and localization of coronary artery disease using nitrogen-13-ammonia. *J Nucl Med* 1993;34:968-978.
 14. Choi Y, Hawkins RA, Huang SC, et al. Parametric images of glucose generated from dynamic cardiac PET and 2-[¹⁸F]Fluoro-2-deoxy-d-glucose studies. *J Nucl Med* 1991;32:733-38.